Atmos. Chem. Phys. Discuss., 13, 15271–15299, 2013
www.atmos-chem-phys-discuss.net/13/15271/2013/
doi:10.5194/acpd-13-15271-2013
© Author(s) 2013. CC Attribution 3.0 License.

Atmospheric Chemistry and Physics Discussions
Open Access

This discussion paper is/has been under review for the journal Atmospheric Chemistry and Physics (ACP). Please refer to the corresponding final paper in ACP if available.

Aerosol variability and atmospheric transport in the Himalayan region from CALIOP 2007–2010 observations

S. Bucci[1,2], C. Cagnazzo[1], F. Cairo[1], L. Di Liberto[1], and F. Fierli[1]

[1]Institute for Atmospheric Sciences and Climate, ISAC-CNR, Italy
[2]Dept. of Physics, Ferrara University, Italy

Received: 18 April 2013 – Accepted: 17 May 2013 – Published: 11 June 2013

Correspondence to: F. Fierli (f.fierli@isac.cnr.it)

Published by Copernicus Publications on behalf of the European Geosciences Union.

Abstract

Himalayan Plateau is surrounded by regions with high natural and anthropogenic aerosol emissions that have a strong impact on regional climate. This is particularly critical for the Himalayan glaciers whose equilibrium is also largely influenced by radiative direct and indirect effects induced by aerosol burden. This work focuses on the spatial and vertical distribution of different aerosol types, their seasonal variability and sources. The analysis of the 2007–2010 yr of CALIPSO vertically resolved satellite data allows the identification of spatial patterns of desert dust and carbonaceous particles in different atmospheric layers. Clusters of Lagrangian back-trajectories highlight the transport pathways from source regions during the dusty spring season. The analysis shows a prevalence of dust; at low heights they are distributed mainly north (with a main contribution from the Gobi and Taklamakan deserts) and west of the Tibetan Plateau (originating from the deserts of South-West Asia and advected by the westerlies). Above the Himalayas the dust amount is minor but still not negligible (detectable in around 20 % of the measurements), and transport from more distant deserts (Sahara and Arabian Peninsula) is important. Smoke aerosol, produced mainly in North India and East China, is subject to shorter range transport and is indeed observed closer to the sources while there is a limited amount reaching the top of the plateau. Data analysis reveals a clear seasonal variability in the frequencies of occurrence for the main aerosol types; dust is regulated principally by the monsoon dynamics, with maxima of occurrence in spring. The study also highlights relevant interannual differences, showing a larger presence of aerosol in the region during 2007 and 2008 yr.

1 Introduction

Aerosol alters the radiative balance through absorption and scattering of the solar radiation (Lau et al., 2006) and influences cloud formation largely impacting the hydrological cycle (Kaufman et al., 2005). More recently, special focus was given to the

ACPD
13, 15271–15299, 2013

aerosol-related climatic processes in the South Asian region where the largest anthropic sources are located and where the presence of desert dust is relevant (Ramanathan et al., 2005; Lau et al., 2008; Bollasina et al., 2008). The fast urban growth and industrialization in the South and East Asia regions has a dramatic impact on the pollutants budget over this area (Lawrence et al., 2011) and was also found to modify the monsoon precipitations and its distribution due to the presence of highly absorbing particulate (Menon et al., 2002; Ramanathan et al., 2007). Layers of air pollution composed by a mixture of aerosol (dust, black carbon, organic carbon and other anthropogenic particulate) were defined as the Atmospheric Brown Clouds (ABC's) (Ramanathan et al., 2005) and they are a persistent feature over South Asia. Aerosol can also modify the microphysical properties of clouds acting as condensation nuclei or influencing the process of water evaporation trough their impact on the radiative budget (Ramanathan et al., 2007). The increased presence of aerosol, especially in late spring, can lead to significant variations on the monsoon evolution and on the hydroclimate of the area: an excess in aerosol load can lead to surface cooling caused by the reduction of incident solar radiation at the surface and increased heating of the troposphere caused by absorption. On the other hand, aerosol can modify the upwelling above the Himalaya with an intensification of the Indian monsoon (the so-called Elevated heat pump or EHP) that is strongly linked to the dust concentration around the plateau during the spring season (Lau et al., 2006). In addition, aerosol can induce a change in cloud amount and precipitation through microphysics (indirect effect) (Menon et al., 2002; Ramanathan et al., 2005; Lau et al., 2006). Moreover, the deposition of particulate on ice and snow affect their surface albedo and ice microphysics (Xu et al., 2009; Krinner et al., 2006) modifying the melting processes. Such variations can be spatially highly inhomogeneous (see for instance Scherler et al. (2011)), suggesting that those changes may be caused by local forcings and, among them, by the variable distribution of particulate. In addiction Bonasoni et al. (2010) shows that strong level of pollutants can affect the South Himalayas especially during the pre-monsoon period and valley circulation may bring also chemicals emitted by local sources up to

cc BY

the plateau. It is hence fundamental to characterize the aerosol spatial distribution and its variability at different timescales and identify its sources. Several recent studies exploited the CALIPSO lidar aerosol observations that give fundamental information on the vertical distribution of airborne particulate; Mishra and Shibata (2012) produced, using aerosol profile data, vertical profiles of aerosol optical properties over the Indo-Gangetic belt, for a time period between June 2006 and December 2009. Kuhlmann and Quaas (2010) estimated the radiative forcing from different types of aerosol above the plateau to discuss the EHP hypothesis while Gautam et al. (2009) characterized the dust burden in the 2007 and 2008 pre-monsoon seasons. Liu et al. (2008) estimated the spatial patterns of desert aerosol in 2007 and highlighted the possible dust transport pathways identifying the plateau as a dynamical obstacle for the westerly jet flow. It is however necessary to investigate also the role of more distant desert areas since some studies evidenced the role of westerly winds during the pre-monsoon season (Bonasoni et al., 2010; Kayetha et al., 2007; Prasad et al., 2006). Liu et al. (2008) with Hysplit back-trajectories showed indeed that the dust found over North Plateau is associated with emissions in the Tarim Basin while in North India it seems to be transported from major deserts of North Eastern India, Pakistan and Afghanistan. The aim of this analysis is twofold. First it provides a characterization of different aerosol type of spatial distribution and seasonal variability based on CALIPSO with an approach similar to what reported in Liu et al. (2008) but extending to observations from 2007 to 2010 and to smoke particulate. Secondly, it presents an assessment of the boundary layer sources for the 2007–2010 pre-monsoon seasons based on Lagrangian numerical simulations.

2 Data and methodology

CALIPSO satellite (Cloud Aerosol Lidar and Infrared Path Finder Satellite, Winker et al., 2007) was developed by NASA and CNES and measures clouds and aerosols from the stratosphere to the ground. It was launched on 28 April 2006 on a sun-

ACPD
13, 15271–15299, 2013

CC BY

synchronous orbit at 705 km of height with 15 orbits per day. CALIPSO hosts the CALIOP lidar (Cloud Aerosol LIdar with Orthogonal Polarization) that operates at 532 nm and 1064 nm wavelengths, and a passive remote sensing instrument working in the infrared bandwidth (IIR, Imaging Infrared Radiometer) and the visible range (WFC, Wide-Field-Camera). Analysis is limited to CALIOP level 2 observations of backscatter vertical profiles to discriminate between clouds and aerosol and to extract local information about their vertical and spatial extent, mean depolarization and backscatter coefficient; optical properties provide a primary discrimination between six different classes of aerosol and eight types of clouds. The analysis focuses on aerosol layers defined in CALIOP data as desert aerosol (dust), particles produced by combustion and composed mainly by soot and organic carbon (smoke), and a mix between dust and smoke (polluted dust) which appear from this analysis to be the main typologies of particulate over the region. Statistics are based on the frequencies of occurrence of each class, estimated as the ratio between the number of observations of at least one layer of a particular class of aerosol and the total number of satellite tracks, within a 3-dimensional grid during a determined time period. The temporal and horizontal resolution of the grid is limited by the repetition rate of the instrument. For a $3^\circ \times 3^\circ$ horizontal resolution CALIOP provides on average 8 to 10 profiles per month. Observations are therefore cumulated over 3 months to have a trade-off between the possibility to have a seasonal coverage and a sufficient number of observations to ensure a reasonable representativeness of each bin. This resolution is compatible to the analysis presented in Liu et al. (2008) where data are accumulated over a $2^\circ \times 2^\circ$ grid. Profiles containing opaque convective or cumulus clouds diagnosed by CALIOP were removed to avoid underestimation of the frequencies of occurrence, computed on a geographical rectangle surrounding the Himalayan Plateau (20° N–45° N, 60° E–120° E) for 2 km thick layers, in the 0 to 8 km height range.

Transport in the region of analysis is estimated calculating daily clusters of back-trajectories that originates from the same rectangle of observational frequencies with an horizontal resolution of 0.5° at two different heights (500 hPa and 700 hPa corre-

Discussion Paper | Discussion Paper | Discussion Paper | Discussion Paper |

ACPD

13, 15271–15299, 2013

Aerosol variability and transport in the Himalayan region

S. Bucci et al.

CC BY

sponding roughly to the 5 and 3 km layer). Trajectories are run backward in time for 10 days to resolve medium range transport patterns, with a reasonable limit on the uncertainty on air parcels position and being compatible with the average lifetime of aerosol in the atmosphere. Meteorological analysis comes from the ECMWF (European Centre for Medium-Range Weather Forecasts, http://www.ecmwf.int/) with 6 h steps and 0.5° resolution. Due to known limits of kinematic trajectories calculation in the turbulent layer, the analysis is limited to the transport above the Planetary Boundary Layer (PBL). So, an approach similar to Bergman et al. (2013) was chosen: sources are identified as the points where the trajectories crossed irreversibly the PBL height, considering the rough approximation that aerosol are uniformly mixed below that layer. The PBL height was estimated accordingly as an idealized terrain-following surface:

$$P_{\mathrm{PBL}} = \frac{0.15 \cdot p^3}{p_0^2} \tag{1}$$

Where p_0 is the mean sea-level pressure. The localization of desert areas was made by means of ground cover maps from US Geological Survey (USGS) Land Cover Institute (LCI) (http://landcover.usgs.gov). Sources of smoke aerosol are identified with the help of MACCity Biomass Burning emissions dataset (http://accent.aero.jussieu.fr/) (Granier et al., 2011; Lamarque et al., 2010; van der Werf et al., 2006). Biomass burning and anthropic emissions of black carbon are cumulated to take into account two main sources of the particles that are classified as smoke based on the observed optical parameters. A minimum threshold of $5 \times 10^{-12}\,\mathrm{kg\,m^{-2}\,s^{-1}}$ is applied to select the more active emission regions. On average, the geographical distribution during the pre-monsoon phase (not reported here) shows the presence of two main macro areas in North India and continental China for anthropic emission, while biomass burning is less intense and more variable in location with frequent production in South-East Asia. A frequency of potential sources was estimated, analogously to CALIPSO aerosol observations, as the ratio between the number of back-trajectories crossing a PBL over a specific source

CC BY

and the number of total back-trajectories for each bin. The result represents a spatial distribution directly comparable with those obtained from CALIOP data.

3 Aerosol variability derived from CALIOP

Spatial distribution of frequency of occurrence for each aerosol class and for each vertical layer is reported in Figs. 1–4 for the winter (DJF), spring (Pre-Monsoon, MAM), summer (Monsoon, JJA) and fall (SON) seasons. Aerosol observations are cumulated over the 2007–2010 yr. In DJF dust occurrences are found south-west and north-east of the plateau in the lower layers with frequencies up to 50 % with a net decrease in the higher layers where, over the eastern part of the plateau, frequencies can reach 20 %. MAM is, on average, richer in dust, forming a similar structure surrounding the plateau in the lower layers with higher frequencies (up to 80 %). In the higher layers the frequency increases above the Plateau with respect to DJF with values that can reach up to 40 % at 4–6 km and 30 % at 6–8 km height. During JJA the distribution is more localized on the western side of the Himalaya. The branch located north of the plateau appears to be weaker and does not reach Eastern China. There is still a relatively important amount of dust that reaches the 6–8 km layer (more than 15 %). In SON the spatial distribution of dust remains largely similar to those observed in summer, with overall lower values of frequency. Nevertheless, bias may arise due to the filtering of convective clouds in Southern India during the Monsoon season, when the scarcity of cloud-free measurements can affect the representativeness of the statistics. As expected, polluted dust shares the distribution of both smoke and dust. A closer look at the CALIPSO backscatter and depolarization profiles for May 2007 (not reported) shows that polluted dust is identified when optical parameters lie in an intermediate range between smoke and dust, thus suggesting that an external mixing of the two species is present without a clear predominance of one specie upon other. Polluted dust in MAM is mostly observed in North India, between the main source regions of dust and carbonaceous particles (respectively Thar and Bay of Bengal). In summer, at

ACPD
13, 15271–15299, 2013

low heights, it is distributed nearly homogeneously over India, China and north-west of the plateau with a frequency around 20 %. In autumn, the frequencies over India increase while decrease on the north-west side. In winter, for the first 2 km, the frequencies over India reach maximum of 70 %, while for the heights between 2 and 4 km the highest frequencies are localized south-east of the plateau. Above the Himalayas there is a nearly steady frequency of slightly less than 10 %, with a maximum in summer.

The results are compared with Liu et al. (2008) where dust is identified as layers with an average aerosol depolarization greater than 0.06 and the aerosol occurrence was determined as the fraction of profiles containing dust with respect to the total number, using cloud-free nighttime data. Although the levels of processing of the database and the time coverage are different, there is a good agreement on the spatial distribution (see plate 2 in Liu et al., 2008). On the other hand, frequencies found here are in general lower than Liu et al. (2008) and largest differences are found for the bottom layer. Discrepancy may be likely attributed to the use of different data and diagnostic applied since level 2 data used here identify the presence of dust with a method that combines an assessment of volume depolarization (that has to be greater than 0.2) and the underlying ground surface type. Moreover level 2 data discriminate between dust and polluted dust, the latter being characterized by a volume depolarization ranging from 0.075 to 0.2. This implies that frequencies reported in Liu et al. (2008) may have a positive bias with respect to the ones presented here. Moreover, orography reduces the vertical thickness of the lowermost layers inducing a possible negative bias on the statistics applied here. This is for example visible in Fig. 2 as a lower frequency area in the 0–2 km layer (with respect to the 2–4 km) around the Thar mountains (65° E, 32° N), where orography is relevant.

Smoke has its maximum values of occurrence in summer. In this season, for the first 4 km atmospheric column, higher frequencies occur east of the plateau, while, during the following season, moves on the South China and North-East India. The pattern remains the same for winter and spring but with a frequencies decrease.

ACPD
13, 15271–15299, 2013

CC BY

In general, dust is the principal typology of aerosol with two distinct main regions (SW and NE Plateau sides) and also relevant presence above the Himalayas. Smoke on the plateau is limited to summer and fall seasons, in both cases with lower frequencies with respect to dust.

Interannual differences are estimated for 4 selected regions: (A) Pakistan and Western India (20° N–33° N, 60° E–81° E) (B) north slopes of the plateau (38° N–42° N, 78° E–102° E) (C) Eastern China (29° N–44° N, 105° E–120° E) and (D) Himalayan Plateau (29° N–38° N, 78° E–102° E). (A) and (B) are two distinct regions rich in dust and polluted dust while (C) presents again high frequencies of both dust and smoke. (D) is needed to evaluate the presence of airborne particles above the Plateau. The frequency timeseries are reported in Fig. 5 and data are now accumulated with a monthly frequency over a three-months wide time window. The time series are estimated for the same layers as Figs. 1–4 but not reported for the regions where orography substantially reduces the layer thickness to avoid a bias on the aerosol frequency of occurrence (0–2 km in North Plateau and China and 0–4 km on the plateau).

In region (A) dust has, at low altitudes, a marked semiannual cycle with two maxima around March and September (the latter is less pronounced). Minima in frequency of occurrence are found in June and November. The presence of an annual cycle at 4–6 km suggests that June minimum in the lower layers can be linked to a mechanical wet deposition during the summer monsoon. Above 6 km there is a significant amount of dust (around 10 %) in Spring and Summer. Is possible to note a clear difference between 2007–2008 and 2009–2010. In these last two years, sensibly lower occurrence of dust aerosol is observed in the lower layers, while highest values are recorded in spring 2008. Gautam et al. (2009) observes a higher dust load in MAM 2008 with respect to 2007 attributing the differences to the increased 2007 winter rainfall on Thar desert region that likely reduced the intensity of the dust source. TRMM (Tropical Rainfall Measurement Mission) monthly mean data available from GPCP (Global Precipitation Climatology Project) show a strong positive precipitation anomaly in spring 2007 while years 2009–2010 appear to be drier (available from GPCP site and not shown

ACPD
13, 15271–15299, 2013

CC BY

here). Our results are therefore consistent with the 2008 maximum aerosol loading of Gautam et al. (2009) but cannot be conclusive on the correlation between low aerosol occurrence and positive anomaly in spring precipitation.

As shown in Fig. 5, India is also the region with highest occurrence of polluted dust reaching values over 30 % between September and December in the first atmospheric layer. Polluted dust occurrence has a marked seasonal variability with a minimum in spring and a maximum in autumn. At higher altitudes the frequencies are lower and the annual cycle is less pronounced. Smoke also presents a well-defined annual periodicity with almost no occurrence in spring, a gradual increase until a maximum of about 6 % in November–December and then a rapid decrease. Presence of smoke above 4 km is marginal. East China (B) is the richest in smoke air with the highest values (on average 10 % of occurrence) in JJA with a similar frequency in the first two layers (even somewhat higher for the 2–4 km). The lower occurrences are observed in March and April. Dust has a maximum in spring as also observed from ground-based AERONET data (Eck et al., 2005). Polluted dust has higher frequencies and an annual cycle close to smoke particles, likely contributing to the maximum optical depth observed in summer by the same authors. North Plateau (C) sees a dominance of dust particles being far from the more intense source regions. The 2–4 km layer shows again a semiannual cycle that is less visible at higher altitudes. Polluted dust and smoke have sensibly lower frequencies of occurrence (a maximum of 10 % and 2 % respectively) with respect to the (A) and (B) regions with a less clear seasonal variability. Himalayan Plateau (D), despite the lower occurrence, has a marked annual cycle for dust and smoke with maxima in spring and summer respectively. Again, 2007 and 2008 are characterized by a higher occurrence of atmospheric particulate.

Overall, as seen before, dust is the dominant type of aerosol on the Himalayan plateau and the surrounding regions. Nevertheless, smoke aerosol and polluted dust have a relevant presence in China and India showing a similar annual cycle that is out of phase with respect to the one followed by dust.

ACPD
13, 15271–15299, 2013

CC BY

4 Aerosol sources and atmospheric transport analysis

The objective is now to identify the possible sources contributing to the observed aerosol spatial distribution and to quantify them as a probability to originate from the PBL above a determined source region. Kinematic back-trajectories were calculated for the dusty spring season (MAM) for 2007–2010. Figure 6 shows the position of air parcels above the PBL originating at 700 hPa east of the Plateau for April 2010 to highlight transport patterns around the Himalayan region. Air masses come from two distinct flows surrounding the plateau. The northern one intercepts potential dust source region from the Taklamakan and Gobi deserts and was identified by Liu et al. (2008) as an airborne dust corridor. The southern one encounters mixed source regions located in West and Northern India (Shrestha and Barros, 2010). It appears that at 700 hPa air parcels exit the PBL mostly locally (light blue points in Fig. 6, left panel) or close to the area where backtrajectories are originated, with a smaller contribution from distant sources. It should be noted that a fraction of air parcels is apparently originating from the PBL above the eastern flank of the plateau leading to a possible overestimate of the PBL contribution. Based on the PBL exit point locations, the main black carbon emission regions are located in the Eastern China and North India, where they seems to influence strongly the amount of pollution in the east side of the plateau with a large number of PBL crossing points over these regions. Similarly dust is principally originated from deserts north of the plateau and, to a lesser extent, more distant sources. At 500 hPa, trajectories indicate that distant sources can have a more important role with respect to 700 hPa with a larger amount of air parcel conveyed by the airborne corridor. PBL exit points are now mostly located above dust sources in Central Sahara, Arabian Peninsula and Iran–Afghanistan while black carbon emissions are intercepted mainly above North India by the southern branch. Figure 7 reports the locations where air parcels ending in the Himalayan region leave irreversibly the PBL. At 700 hPa (roughly representative of the 2–4 km layer) more than 57 % of the air masses comes from the PBL with a dominance of sources included in the larger Himalayan

ACPD
13, 15271–15299, 2013

region. Desert sources account for nearly 23 % with more than one third (around 8 %) coming from arid areas north of the plateau (Gobi and Taklamakan) while the remaining fraction originates from Thar, Iranian and Arabian deserts. Trajectories coming from biomass burning sources contribute up to 8.5 % and are distributed over the main region of emissions: Eastern China and, to a less extent, North India. At 500 hPa (4–6 km) the trajectories coming from PBL are 24.4 % of the total with a different spatial distribution: dust is linked to a longer range transport, coming now from the Arabian Peninsula and the Sahara. Desert dust trajectories now contribute up to half of the total PBL air (12.8 % of the total), with a much smaller fraction (2.1 % of the total) coming from Gobi and Taklamakan. Air masses from biomass burning area are also a smaller fraction (2.6 %) with respect to the 700 hPa layer. The PBL crossing points are located over the main emissions regions but, with respect to the 700 hPa layer, North India sources spans over a larger area. The same estimates were done for each year from 2007 to 2010 and it appears that there are no significant inter-annual variations in the PBL sources fractions. The values reported in Fig. 7 may be directly compared with the regional mean of the occurrence frequency derived from CALIPSO data in Fig. 2. This is based on the assumption that the probability to observe the presence of an aerosol layer (that can be thin) can be quantitatively explained by the probability of transport from aerosol sources given by the Lagrangian analysis. Despite the fact that this assumption can be straightforward, significant differences may occur, besides the error of the Lagrangian transport itself, from several factors of uncertainty. Circulation given by the atmospheric analysis is not representative of mesoscale processes that influence aerosol distribution (i.e. forced uplift, local convection); the assumption of pure passive transport neglects the removal processes; the source attribution does not take into account the uncertainty of the emissions and their degree of vertical mixing inside the PBL that may affect the effective dust or biomass burning load at the top of it. In addition, observed polluted dust cannot be partitioned into smoke and dust aerosol since both sources may contribute to its formation (this is visible in Fig. 2 above North India). Therefore, in the following analysis, it is decided to only consider pure dust and

CC BY

smoke in order to avoid multiple countings and hence an overestimate of the observed frequency of layer detection. CALIPSO at 700 hPa (2–4 km) gives a frequency of dust occurrence of 26 % and about 4 % of smoke (with 10 % of polluted dust). Despite the uncertainties mentioned above, such values are in satisfactory agreement with those derived from the trajectories. Similarly, at 500 hPa (4–6 km) the observed frequencies of occurrence (dust 14.3 % and smoke 1.5 %) are comparable to those derived from the Lagrangian analysis. Figure 8 reports the fraction of backtrajectories originating from the whole PBL and the source regions identified before (deserts and carbonaceous emissions in South-Asia). Their spatial distribution may be compared directly with the observations reported in Fig. 2. At 700 hPa particles coming from the PBL show a nearly homogeneous distribution around the Plateau with a maximum in the south-east side. This area presents modest orography and therefore a higher PBL top (in geographical coordinates) with respect to the surrounding regions. Consequently a back-trajectory leaving from that area has a greater probability to have a close encounter with the PBL, leading to higher frequencies in its geographical distribution. Moreover, the overestimate of the PBL air east of the plateau may come from a flux originating on the Eastern flank of the Himalaya (see discussion of Fig. 6). PBL exit is co-located with a high emissive region leading to a likely overestimate of smoke maximum occurrence. Besides this anomaly, smoke frequencies are substantially similar to those derived from CALIPSO (around 20 %). Trajectories analysis shows that smoke emissions mainly impact a region south-east of the plateau (between North India and East China) that is identified in the observations, the latter showing also a relevant region south of the Himalaya where emissive fluxes are negligible (as visible in Fig. 6). Again, this difference may be attributed to an incorrect transport in the PBL and/or to the emissions used that includes anthropogenic biomass and biomass burning while the smoke identified in CALIPSO may comprehend a larger typology of pollutants. The spatial distribution of observed dust aerosol is correctly reproduced by the transport diagnostics. The frequency of occurrence is also generally well represented, with values slightly smaller than the observed ones. The dusty region north of the plateau is cor-

ACPD
13, 15271–15299, 2013

rectly identified and it appears to be mainly linked to aerosol transport from Gobi and Taklamakan. Western pattern of dust comes from longer range transport, with a relevant contribution from Sahara and Arabian Peninsula. Satellite observations show a more pronounced penetration of dusty layers south-east of the plateau. At 500 hPa (Fig. 9), the trajectories seem to have less agreement with the observations. It is necessary to note that ECMWF analysis give a wind field at 500 hPa (representative of the 4–6 km layer) that is almost similar to the 450 hPa and 400 hPa levels (not shown); so, the pattern reproduced by Lagrangian analysis may be qualitatively compared to the observations in the higher layers. This confirms the presence of a W–E pattern above the Himalayan region. Coming back to the 500 hPa levels, despite a substantial agreement for the total frequencies (around 20 % in both simulation and measurements), the spatial distribution shows several discrepancies. Trajectories indicates a main dust belt north (and partially above) the plateau while measurement, in addition to this pattern, shows an accumulation of dust aerosol on the south-west flank, similarly to the 700 hPa layer. The discrepancy can be again attributed to a bias coming from the vertical resolution of the wind fields that, at 500 hPa, makes the influence of the mechanical obstacle of the plateau less relevant with respect to the real atmospheric circulation. Moreover, the contribution of the high level jet may be overestimated leading to a more efficient westerly transport. There is still a small amount of dust coming from the local deserts that can reach the northern side of the Himalayan Plateau but, at this height, its contribution is less relevant. Smoke is found with similar percentages than in the observations but, as for the 700 hPa layer, is located slightly north to the measurements.

5 Conclusions

The CALIOP lidar satellite-borne observations in the Himalaya region allow the analysis of the spatial distribution and the seasonal and monthly variability of different forms of atmospheric aerosol, identified on the basis of the observed optical parameters. Aerosol is quantified as the number of occurrences of a single particle layer on a reg-

ACPD
13, 15271–15299, 2013

ular 3-D grid on seasonal basis; it is normalized to the total number of observations to provide the probability to observe a determined type of atmospheric particulate that can be directly compared to model-derived diagnostics. Dust is the more probable type in the wider Himalayan Plateau region with a marked seasonal cycle, with a maximum in spring. During this season, occurrence of dust may reach 75 % of observations. Smoke particles have a lower occurrence with a maximum during summer season (reaching around 25 %). Trajectories cluster analysis is used to quantify the role of different distant sources on the aerosol load over the region and their spatial distribution. This is directly compared to the observed occurrence frequency and, in general, a satisfactory agreement is found, supporting the use of Lagrangian calculations for the interpretation of the observed aerosol patterns. Discrepancies seem to arise from limitations of the transport (limited vertical resolution, uncertainty on emissions, inaccuracy of transport pattern leeward of the plateau). Concerning the spatial distribution, it is found that dust is observed preferentially south-west and north of the plateau. A not negligible amount of aerosol reaches above the plateau: dust is found over the peaks with a frequency reaching about 20 % of the observations in spring. Polluted dust and smoke are observed over the plateau mainly in summer with lower values of occurrence (maximum 10 % and 5 % respectively). Transport analysis shows that in the lower atmospheric layers dust particles originates from closer sources (Taklamakan and Gobi for the northern area and south central Asia for the southern area). During spring, when dust has its maximum, transport occurs through the pattern of a W–E corridor surrounding the plateau and dividing in two branches. The northern branch goes towards the northern side of the plateau with a maximum eastward extension in spring, and is fed by dust coming from the local deserts with a likely role in determining the maximum dust occurrence above China during spring season. Smoke particles, mainly emitted in North India and China, can be partly conveyed by the southern branch and are preferentially observed in south-east of the Plateau, where strong sources are present. The annual variability of the smoke occurrence is related to the cycle of emissions of anthropogenic and biomass burning that has a maximum in China during summer, while dust occur-

ACPD
13, 15271–15299, 2013

CC BY

rence in North India is, as expected, modulated by the seasonality of the monsoon. The general features of the aerosol spatial distribution are coherent for different atmospheric levels with a decrease in occurrence of observations above 4 km height where the westerly flow seems to have a more effective role. Lagrangian analysis indicates that a substantial fraction of dust particles may originate from PBL above the Arabian and Sahara deserts and is subsequently advected north of the plateau. Similarly, the transport in the southern branch is also more intense, leading to a more efficient westerly advection from north India sources. CALIOP also provides observations of a mixed aerosol type (the so-called polluted dust) that is characterized by values of optical parameters intermediate between smoke and dust. It is mainly observed in North India where, based on the above conclusions, it is expected a coexistence of dust advected from western sources and smoke originated locally. The value of occurrence of polluted dust, in general, lies between those found for the two other types while its annual cycle is often less marked, nonetheless with a behavior similar to the smoke aerosol. The presence of aerosol above the plateau is important, especially for dust, with a marked annual cycle for both desert aerosol and smoke particles. Despite the limited length of the observational timeseries, it is possible to clearly identify differences in aerosol occurrence among the four years. 2007 and 2008 have larger observational frequencies for each of the aerosol types throughout the region. The underlying mechanism is not fully clarified; transport does not show any clear differences between the high and low occurrence years. Similarly, inter-annual differences in precipitation above source regions during the pre-monsoon season cannot explain a possible modulation of the intensity of dust sources. Overall, the analysis presented here provides an extension of the intra-seasonal dust characterization reported in previous works, giving an assessment of the variability of different particle types and identifying marked inter-annual differences. Lagrangian analysis supported the identification of the main transport patterns, highlighting the possible role of long-range transport in dust distribution in the Himalayan plateau region. The diagnostics derived from observations on a regular geographical grid may also be directly compared to global aerosol model output, in order

ACPD
13, 15271–15299, 2013

cc BY

to quantify their ability in reproducing aerosol distribution, its variability and the possible sources in the hot spot climatic region of the Himalayan Plateau.

Acknowledgements. The work is partly funded by the EVK2-Share project Paprika. CALIPSO data were obtained from the NASA Langley Research Center Atmospheric Science Data Center. MACCity emissions come from the ECCAD program. ECMWF data used in this study have been obtained from the ECMWF Data Server.

References

Bergman, J. W., Fierli, F., Jensen, E. J., Honomichl, S., and Pan, L. L.: Boundary layer sources for the Asian anticyclone: Regional contributions to a vertical conduit, J. Geophys. Res. Atmos., 118, 2560–2575, doi:10.1002/jgrd.50142, 2013. 15276

Berthier, E., Arnaud, Y., Kumar, R., Ahmad, S., Wagnon, P., and Chevallier, P.: Remote sensing estimates of glacier mass balances in the Himachal Pradesh (Western Himalaya, India), Remote Sens. Environ., 108, 327–338, 2007.

Bollasina, M., Sumant, N., and Lau, K.-M.: Absorbing aerosols and summer monsoon evolution over South Asia: an observational portrayal, J. Climate, 21, 3221–3239, doi:10.1175/2007JCLI2094.1, 2008. 15273

Bonasoni, P., Cristofanelli, P., Marinoni, A., Pradhan, B. B., Fuzzi, S., Gobbi, G. P., Vuillermoz, E., and Laj, P.: High concentration of black carbon observed in the high himalayas, UNEP Black Carbon E-bulletin, Volume 2, Number 2, July 2010. 15273, 15274

Das, S. K., Dobhal, D. P., and Juyal, N.: Variability of aerosol optical depth and recent recessional trend in Dokriani Glacier, Bhagirathi Valley, Garhwal Himalaya, Curr. Sci. India, 99, 1816–1821, 2010. Diehl, T., Heil, A., Chin, M., Pan, X., Streets, D., Schultz, M., and Kinne, S.: Anthropogenic, biomass burning, and volcanic emissions of black carbon, organic carbon, and SO_2 from 1980 to 2010 for hindcast model experiments, Atmos. Chem. Phys. Discuss., 12, 24895–24954, doi:10.5194/acpd-12-24895-2012, 2012.

Eck, T. F., B. N. Holben, O. Dubovik, A. Smirnov, P. Goloub, H. B. Chen, B. Chatenet, L. Gomes, X.-Y. Zhang, S.-C. Tsay, Q. Ji, D. M. Giles, and I. Slutsker: Columnar aerosol optical properties at AERONET sites in central eastern Asia and aerosol transport to the tropical mid-Pacific, J. Geophys. Res., 110, D06202, doi:10.1029/2004JD005274., 2005 15280

CC BY

Gautam, R., Hsu, N. C., Gautam, R., Hsu, N. C., Lau, K.-M., Tsay, S.-C., and Kafatos, M.: Enhanced pre-monsoon warming over the Himalayan-Gangetic region from 1979 to 2007, Geophys. Res. Lett., 36, L07704, doi:10.1029/2009GL037641, 2009. 15274, 15279, 15280

Granier, C., Bessagnet, B., Bond, T. C., D'Angiola, A., Denier van der Gon, H., Frost, G. J., Heil, A., Kaiser, J. W., Kinne, S., Klimont, Z., Kloster, J., Lamarque, J. F., Liousse, C., Masui, T., Meleux, F., Mieville, A., Ohara, T., Raut, J. C., Riahi, K., Schultz, M., Smith, S. J., Thomson, A. M., van Aardenne, J., van der Werf, G. R., and Van Vuuren, D.: Evolution of anthropogenic and biomass burning emissions of air pollutants at global and regional scales during the 1980–2010 period, Clim. Change, 109, 163–190, doi:10.1007/s10584-011-0154-1, 2011. 15276

Kayetha, V. K., Kumar J. S., Prasad, A. K., Cervone, G., and Singh, R. P.: Effect of dust storm on ocean color and snow parameters, Journal of the Indian Society of Remote Sensing, 35, 1–9, doi:10.1007/BF02991828, 2007. 15274

Lamarque, J.-F., Bond, T. C., Eyring, V., Granier, C., Heil, A., Klimont, Z., Lee, D., Liousse, C., Mieville, A., Owen, B., Schultz, M. G., Shindell, D., Smith, S. J., Stehfest, E., Van Aardenne, J., Cooper, O. R., Kainuma, M., Mahowald, N., McConnell, J. R., Naik, V., Riahi, K., and van Vuuren, D. P.: Historical (1850–2000) gridded anthropogenic and biomass burning emissions of reactive gases and aerosols: methodology and application, Atmos. Chem. Phys., 10, 7017–7039, doi:10.5194/acp-10-7017-2010, 2010. 15276

Lau, K. M., Kim, M. K., and Kim, K. M.: Asian summer monsoon anomalies induced by aerosol direct forcing: the role of the Tibetan Plateau, Clim. Dynam., 26, 855–864, doi:10.1007/s00382-006-0114-z, 2006. 15272, 15273

Lau, K.-M., Ramanathan, V., Wu, G.-X., Li, Z., Tsay, S. C., Hsu, C., Sikka, R., Holben, B., Lu, D., Tartari, G., Chin, M., Koudelova, P., Chen, H., Ma, Y., Huang, J., Taniguchi, K., and Zhang, R.: The Joint Aerosol-Monsoon Experiment: A new Challenge for monsoon climate research, B. Am. Meteor. Soc., 89, 369–383, doi:10.1175/BAMS-89-3-369, 2008. 15273

Lau, W. K. M., Kim, M.-K., Kim, K.-M., and Lee, W.-S.: Enhanced surface warming and accelerated snow melt in the Himalayas and Tibetan Plateau induced by absorbing aerosols, Environ. Res. Lett., 5, 025204, doi:10.1088/1748-9326/5/2/025204, 2010.

Lawrence, M. G.: Atmospheric science: Asia under a high-level brown cloud, Nat. Geosci, 4, 352–353, 2011. 15273

CC BY

Liu, D., Wang, Z., Liu, Z., Winker, D., and Trepte, C.: A height resolved global view of dust aerosols from the first year CALIPSO lidar measurements, J. Geophys. Res., 113, D16214, doi:10.1029/2007JD009776, 2008. 15274, 15275, 15278, 15281

Liu, X. D. and Chen, B. D.: Climatic warming in the Tibetan Plateau during recent decades, Int. J. Climatol., 20, 1729–1742, 2000.

Kaufman, Y. J., Tanre, D., and Boucher, O.: A satellite view of aerosols in the climate system, Nature, 419, 215–223, 2002. 15272

Krinner, G., Boucher, O., and Balanski, Y.: Ice-free glacial northern Asia due to dust deposition on snow, Clim. Dynam., 27, 773–777, 2006. 15273

Kuhlmann, J. and Quaas, J.: How can aerosols affect the Asian summer monsoon? Assessment during three consecutive pre-monsoon seasons from CALIPSO satellite data, Atmos. Chem. Phys., 10, 4673–4688, doi:10.5194/acp-10-4673-2010, 2010. 15274

Menon, S., Hansen, J., and Nazarenko, L.: Climate effects of black carbon aerosols in China and India, Science, 297, 2250–2253, 2002. 15273

Mishra, A. K. and Shibata, T.: Climatological aspects of seasonal variation of aerosol vertical distribution over central Indo-Gangetic belt (IGB) inferred by the space-borne lidar CALIOP, Atmos. Environ., 46, 365–375, 2012. 15274

Prasad, A. K., Singh, R. P., and Singh, A.: Seasonal climatology of aerosol optical depth over the Indian subcontinent: trend and departures in recent years, Int. J. Remote Sens., 27, 2323–2329, 2006. 15274

Prasad, A. K., Singh, S., Chauhan, S. S., Srivastava, M. K., Singh, R. P., and Singh, R.: Aerosol radiative forcing over the Indo-Gangetic plains during major dust storms, Atmos. Environ., 41, 6289–6301, 2007.

Prasad, A. K., Yang, K.-H. S., El-Askary, H. M., and Kafatos, M.: Melting of major Glaciers in the western Himalayas: evidence of climatic changes from long term MSU derived tropospheric temperature trend (1979–2008), Ann. Geophys., 27, 4505–4519, doi:10.5194/angeo-27-4505-2009, 2009.

Ramanathan, V. and Carmichael, G.: Global and regional climate changes due to black carbon, Nat. Geosci., 1, 221–227, 2008.

Ramanathan, V., Crutzen, P. J., Lelieveld, J.,Mitra, A. P., Althausen, D., Andersons, J., Andreae, M. O., Cantrell, W., Cass, G. R., Chung, C. E., Clarke, A. D., Coakley, J. A., Collins, W. D., Conant, W. C., Dulac, F., Heintzenberg, J., Heymsfield, A. J., Holben, B., Howell, S., Hudson, J., Jayaraman, T. A., Kiehl, J. T., Krishnamurti, T. N., Lubin, D., McFarquhar, G., Novakov, T.,

ACPD
13, 15271–15299, 2013

Aerosol variability and transport in the Himalayan region

S. Bucci et al.

CC BY

Ogren, J. A., Podgorny, I. A., Prather, K., Priestley, K., Prospero, J. M., Quinn, P. K., Rajeev, K., Rasch, P., Rupert, S., Sadourny, R., Satheesh, S. K., Shaw, G. E., Sheridan, P., and Valero, F. P. J.: Indian ocean experiment: an integrated analysis of the climate forcing and effects of the great Indo-Asian haze, J. Geophys. Res., 106, 28371–28399, 2001.

Ramanathan, V., Chung, C., Kim, D., Bettge, T., Buja, L., Kiehl, J. T., Washington, W. M., Fu, Q., Sikka, D. R., and Wild, M.: Atmospheric brown clouds: Impacts on South Asian climate and hydrological cycle, P. Natl. Acad. Sci. USA, 102, 5326–5333, doi:10.1073/pnas.0500656102, 2005. 15273

Ramanathan, V., Li, F., Ramana, M. V., Praveen, P. S., Kim, D., Corrigan, C. E., Nguyen, H., Stone, E. A., Schauer, J. J., Carmichael, G. R., Adhikary, B., and Yoon, S. C.: Atmospheric brown clouds: Hemispherical and regional variations in long-range transport, absorption, and radiative forcing, J. Geophys. Res., 112, D22S21, doi:10.1029/2006JD008124, 2007. 15273

Scherler, D., Bookhagen, B., and Strecker, M. R.: Spatially variable response of Himalayan glaciers to climate change affected by debris cover, Nature Geosci., 4, 156–159, doi:10.1038/ngeo1068, 2011. 15273

Shrestha, P. and Barros, A. P.: Joint spatial variability of aerosol, clouds and rainfall in the Himalayas from satellite data, Atmos. Chem. Phys., 10, 8305–8317, doi:10.5194/acp-10-8305-2010, 2010. 15281

Singh, R. P., Dey, S., Tripathi, S. N., Tare, V., and Holben, B.: Variability of aerosol parameters over Kanpur, northern India, J. Geophys. Res.-Atmos., 109, D23206, doi:10.1029/2004JD004966, 2004.

van der Werf, G. R., Randerson, J. T., Giglio, L., Collatz, G. J., Kasibhatla, P. S., and Arellano Jr., A. F.: Interannual variability in global biomass burning emissions from 1997 to 2004, Atmos. Chem. Phys., 6, 3423–3441, doi:10.5194/acp-6-3423-2006, 2006. 15276

Winker, D. M., Hunt, W. H., and McGill, M. J.: Initial performance assessment of CALIOP, Geophys. Res. Lett., 34, L19803, doi:10.1029/2007gl030135, 2007. 15274

Xu, B., Cao, J., Hansen, J., Yao, T., Joswia, D. J., Wang, N., Wu, G., Wang, M., Zhao, H., Yang, W., Liu, X., and He, J.: Black soot and the survival of Tibetan glaciers, P. Natl. Acad. Sci. USA, 106, 22114–22118, doi:10.1073/pnas.0910444106, 2009. 15273

Zhang, X., Cao, J., An, Z., and Wang, D.: Atmospheric dust aerosol over the Tibetan Plateau, J. Geophys. Res., 106, 18471–18476, doi:10.1029/2000JD900672, 2001.

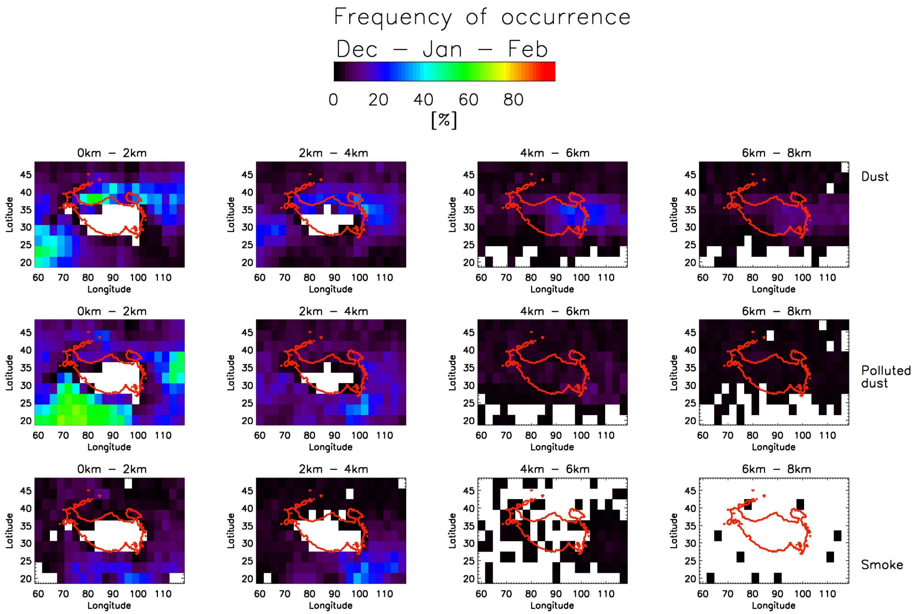

Fig. 1. Aerosol frequency of occurrence for the DJF season. Different aerosol types (dust, polluted dust, smoke) are reported from top to bottom. Different vertical layers are reported from left to right.

ACPD
13, 15271–15299, 2013

Aerosol variability and transport in the Himalayan region

S. Bucci et al.

Title Page
Abstract Introduction
Conclusions References
Tables Figures
◂ ▸
Back Close
Full Screen / Esc
Printer-friendly Version
Interactive Discussion

CC BY

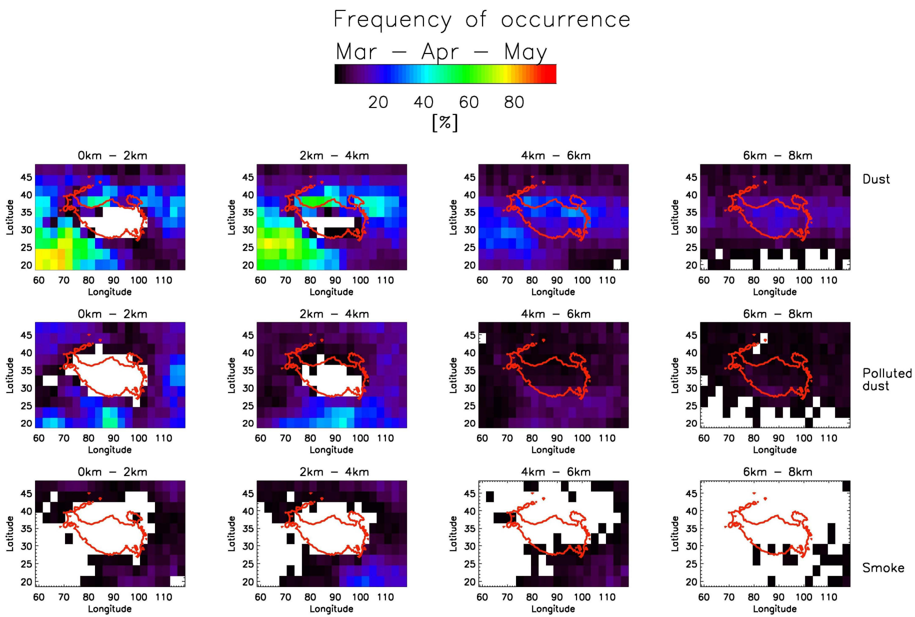

Fig. 2. As Fig. 1 but for MAM season.

CC BY

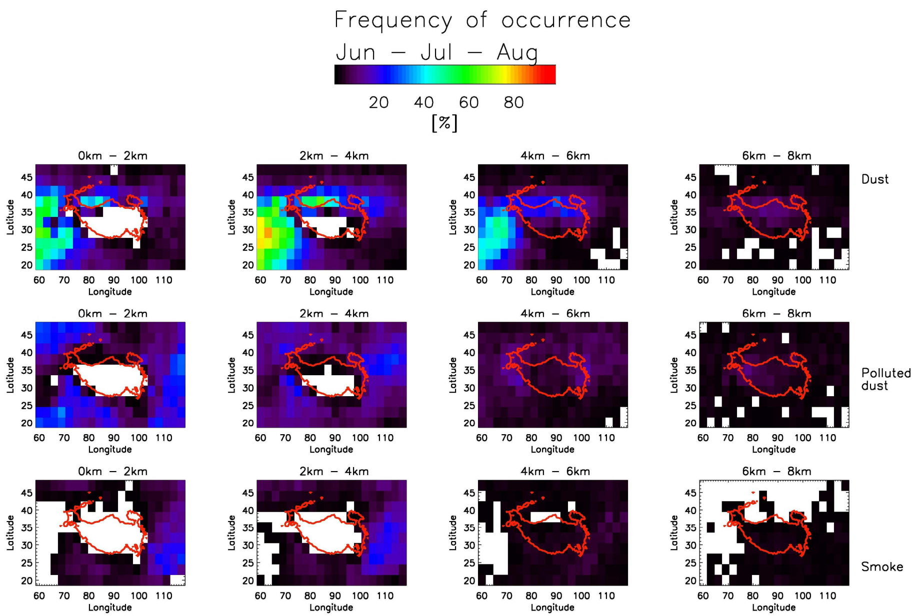

Fig. 3. As Fig. 1 but for JJA season.

ACPD
13, 15271–15299, 2013

CC BY

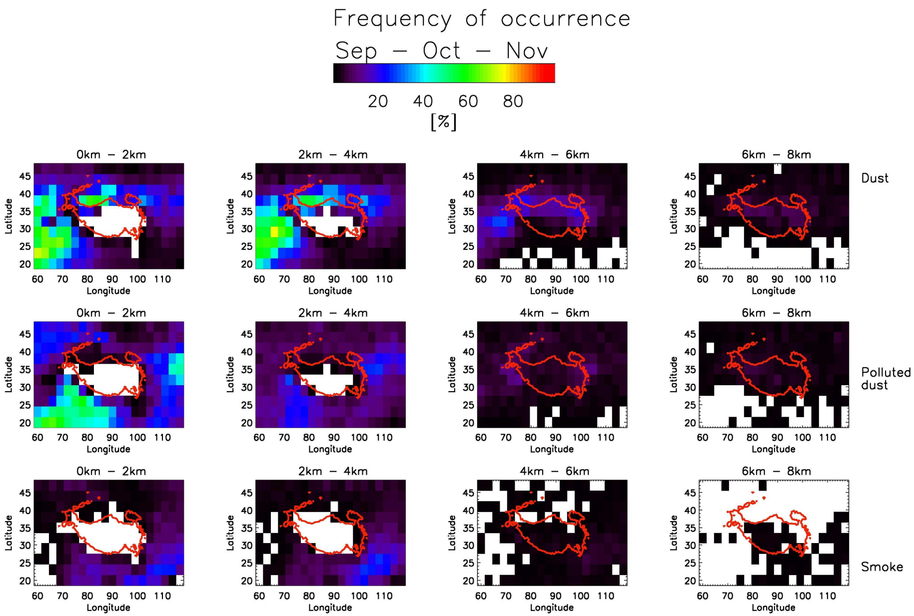

Fig. 4. As Fig. 1 but for SON season.

CC BY

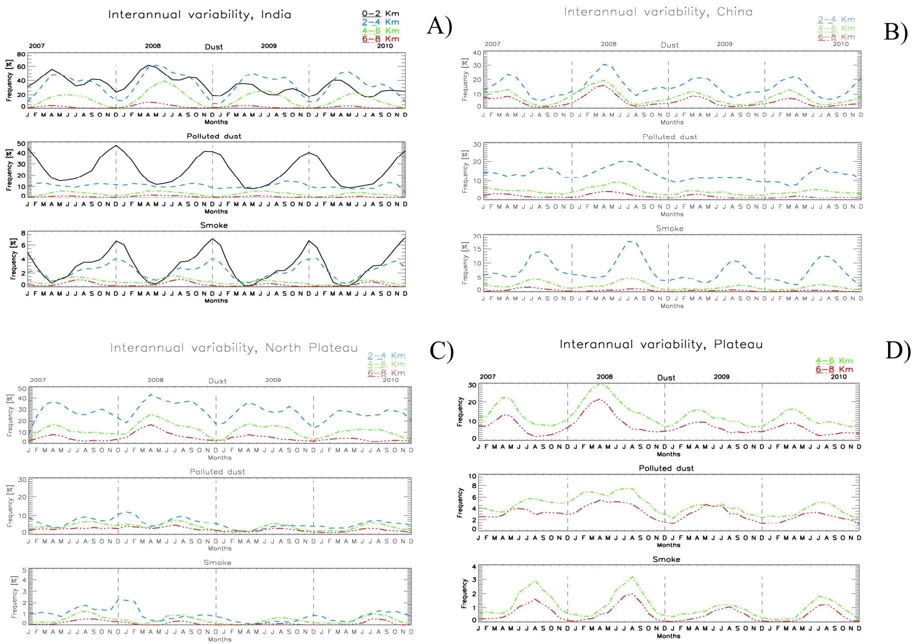

Fig. 5. Frequency of occurrence for dust, polluted dust and smoke for the A, B, C, D regions (as defined in the text) for the years 2007–2010. Different lines report the vertical layers 0–2 km (black), 2–4 km (blue dashed), 4–6 km (green), 6–8 km (red). Readers may note the different vertical scales.

CC BY

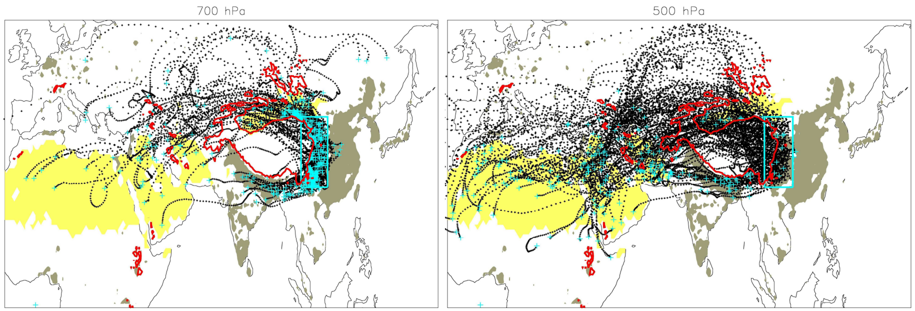

Fig. 6. Back-trajectories originating east of the plateau at 700 hPa (left) and 500 hPa (right) for April 2010. Light blue box indicates the starting point area of the back trajectories. Yellow areas are the dust regions considered as potential sources. Grey areas are total black carbon emissions greater than the threshold in the text. Back-trajectories patterns are represented by the black dotted lines, while the light blue points are the irreversible PBL crossing points. Red contour reports the 700 hPa level to identify the presence of the Himalayan Plateau.

ACPD
13, 15271–15299, 2013

Aerosol variability and transport in the Himalayan region

S. Bucci et al.

CC BY

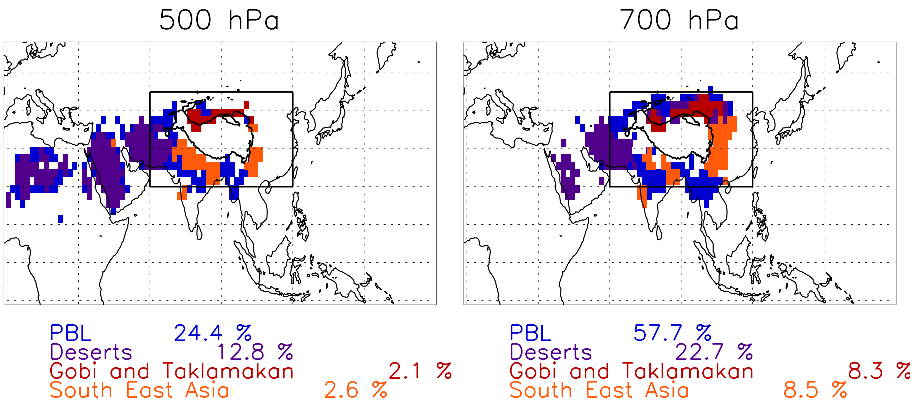

Fig. 7. Geographical distribution of PBL exit points for backtrajectories at 500 hPa (left) and 700 hPa (right). Different sources are plotted with the color table reported in the figure together with its relative contribution. Black box indicates the starting point area of the back-trajectories. Analysis includes the 2007–2010 spring seasons.

ACPD
13, 15271–15299, 2013

Aerosol variability and transport in the Himalayan region

S. Bucci et al.

CC BY

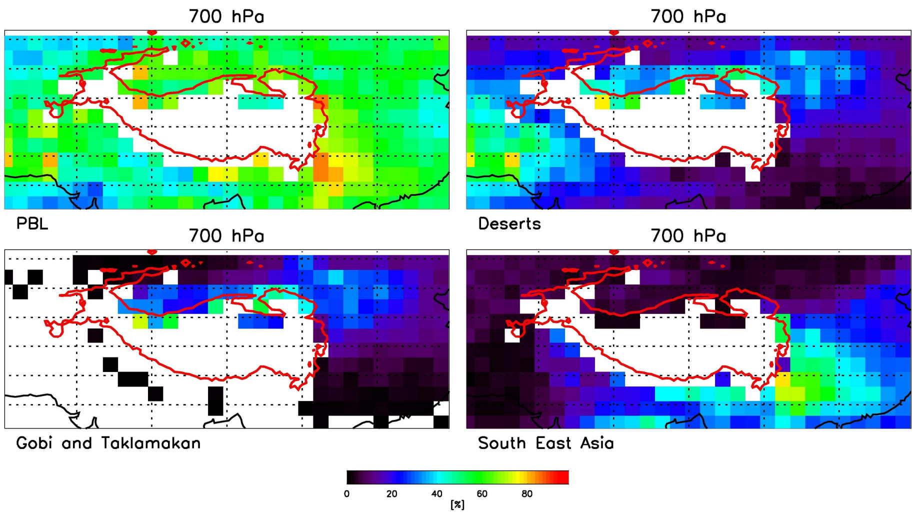

Fig. 8. Frequency of occurrence of air masses at 750 hPa coming from different PBL sources (top left panel whole PBL as defined in the text, top right PBL above deserts, bottom left PBL above deserts north of the plateau, bottom right PBL above carbon aerosol emissive regions). Color scale is the same as Figs. 1–4.

ACPD
13, 15271–15299, 2013

CC BY

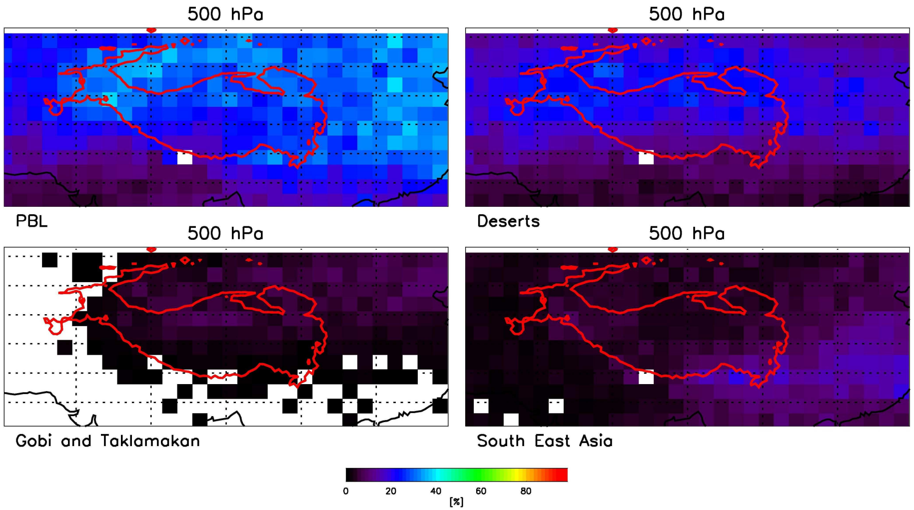

Fig. 9. As Fig. 8 but for the 500 hPa level.

ACPD
13, 15271–15299, 2013

Aerosol variability and transport in the Himalayan region

S. Bucci et al.

cc BY